Energy management system optimization based on an LSTM deep learning model using vehicle speed prediction

Transportation Engineering 11 (2023) 100160

Contents lists available at ScienceDirect

Transportation Engineering

journal homepage: www.sciencedirect.com/journal/transportation-engineering

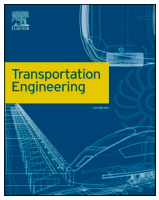

Energy management system optimization based on an LSTM deep learning model using vehicle speed prediction

Luca Pulvirenti, Luciano Rolando *, Federico Millo

Politecnico di Torino, C.so Duca Degli Abruzzi, 24, Turin, (TO) 10129, Italy

ARTICLE INFO

Keywords:
Hybrid Electric Vehicle
Energy management system
Vehicle connectivity
LSTM deep learning
Adaptive ECMS

ABSTRACT

The energy management of a Hybrid Electric Vehicle (HEV) is a global optimization problem, and its optimal solution inevitably entails knowing the entire mission profile. The exploitation of Vehicle-to-Everything (V2X) connectivity can pave the way for reliable short-term vehicle speed predictions. As a result, the capabilities of conventional energy management strategies can be enhanced by integrating the predicted vehicle speed into the powertrain control strategy. Therefore, in this paper, an innovative Adaptation algorithm uses the predicted speed profile for an Equivalent Consumption Minimization Strategy (A-V2X-ECMS). Driving pattern identification is employed to adapt the equivalence factor of the ECMS when a change in the driving patterns occurs, or when the State of Charge (SoC) experiences a high deviation from the target value. A Principal Component Analysis (PCA) was performed on several energetic indices to select the ones that predominate in characterizing the different driving patterns. Long Short-Term Memory (LSTM) deep neural networks were trained to choose the optimal value of the equivalence factor for a specific sequence of data (i.e., speed, acceleration, power, and initial SoC). The potentialities of the innovative A-V2X-ECMS were assessed, through numerical simulation, on a diesel Plug-in Hybrid Electric Vehicle (PHEV) available on the European market. A virtual test rig of the investigated vehicle was built in the GT-SUITE software environment and validated against a wide database of experimental data. The simulations proved that the proposed approach achieves results much closer to optimal than the conventional energy management strategies taken as a reference.

1. Introduction

Climate change and the depletion of natural resources pose existential threats to the whole planet. To address these challenges, Regulators are imposing increasingly stringent limitations in terms of CO_2 and pollutant emissions. Focusing on Europe, the European Commission (EC) is proposing a transformation of the European Union (EU) economy and society to meet climate goals: the European Green Deal aims to transform the EU into a modern, resource-efficient, and competitive economy, ensuring, among the targets, zero net emissions of Greenhouse gases (GHGs) by 2050 [1]. In this framework, on July 14, 2021, the EC put forward the "Fit for 55" regulatory proposals intended to secure an EU economy-wide GHG reduction of at least 55% by 2030, compared to 1990 levels [2]. Since transport is one of the most energy-intensive sectors (in 2018 it accounted for 35% of the worldwide energy consumption [3]), one of the regulatory proposals adopted by the EC is to amend the CO_2 emission targets for new passenger cars and light commercial vehicles. The EC proposal lowers the current 2030 CO_2 targets,

Abbreviations: A-ECMS, adaptive ECMS; AT, automatic transmission; A-V2X-ECMS, adaptive ECMS based on V2X connectivity; BEV, battery electric vehicle; BMEP, brake mean effective pressure; BMS, battery management system; BSFC, brake specific fuel consumption; CAV, connected and automated vehicle; CD, charge depleting; CNN, convolution neural network; CPU, central processing unit; CS, charge sustaining; DC, direct current; DNN, deep neural network; ECMS, equivalent consumption minimization strategy; EC, European commission; ECU, electronic control unit; EM, electric machine; EMS, energy management system; EU, European union; FFT, fast fourier transform; GHG, greenhouse gas; GPS, global positioning system; HEV, hybrid electric vehicle; HV, high voltage; ICE, internal combustion engine; ITS, intelligent transportation system; LiNMC, Li-Ion Nickel-manganese-cobalt-oxide; LPM, load point moving; LSTM, long short-term memory; LV, low voltage; NEDC, new European driving cycle; NN, neural network; OOL, optimal operating line; PCA, principal component analysis; PEMS, portable emissions measurement system; PHEV, plug-in hybrid electric vehicle; PID, proportional–integral–derivative; RDE, real driving emission; RNN, recurrent neural network; RT, real-time; SoC, state of charge; V2X, vehicle-to-everything; WLTC, worldwide harmonized light-duty cycle; ZEV, zero-emission vehicle.

* Corresponding author.
E-mail address: luciano.rolando@polito.it (L. Rolando).

https://doi.org/10.1016/j.treng.2023.100160
Received 6 October 2022; Received in revised form 28 December 2022; Accepted 3 January 2023
Available online 4 January 2023

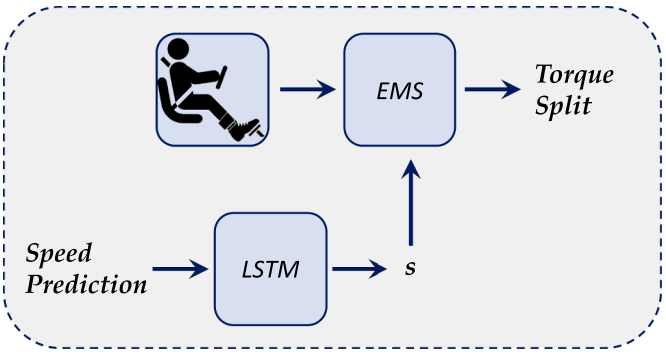

Fig. 1. Layout of the proposed methodology: vehicle speed prediction is used by an LSTM network to assign the optimal equivalence factor for an ECMS.

from −37.5% to −55% for new passenger cars and from −31% to −50% for new vans, both relative to 1990 levels. In addition, the proposal introduces an even more challenging target for 2035: a 100% reduction of CO_2 emissions for new cars and vans, again relative to 1990 levels. Instead, the 2025 CO_2 target remains unchanged at −15% for both new cars and vans [4].

For vehicle manufacturers, the best option to achieve compliance with current legislation targets and future proposals is by electrifying their product portfolio. This approach seems to be one of the most promising solutions since the legislative framework is currently based on a tank-to-wheels approach, i.e., it only takes into account tailpipe emissions, considering Battery Electric Vehicles (BEVs) as Zero-Emission Vehicles (ZEVs). The increased offer of electrified vehicles from manufacturers along with the incentives and benefits provided by the member states of the EU for buying or owning an electrified car [5], has led to the unprecedented growth of electrified vehicle sales in the European market. Although in 2020 the sales of all new cars in the EU fell by 20% due to COVID-19, a 143% increase, relative to 2019, was recorded in the electrified vehicles market [6]. This led to a 21% decrease in the average new vehicle type approval CO_2 emissions in Europe relative to 2019 levels [7]. Although the BEVs market is experiencing remarkable growth (5.4% share of new cars sold in the EU in 2020 [8]), their limited range, long recharging times, and inadequate infrastructure, still make Hybrid Electric Vehicles (HEVs) and Plug-in Hybrid Electric Vehicles (PHEVs) the preferred solution in a mid-term scenario [9], since they can combine the desired features of electric and conventional powertrains.

However, HEV fuel economy is highly dependent on the cooperation between the Internal Combustion Engine (ICE) and the Electric Machines (EMs) installed on board. An additional level, namely the Energy Management System (EMS), has to be added to the vehicle control hierarchy to optimize the energy flows in the powertrain through a proper definition of the power split between the available power actuators [10]. A remarkable amount of research into EMS has been conducted over the last decade: according to [11], the existing EMSs can be broadly classified as Rule-Based (RB), optimization-based, and learning-based. Among the optimization-based techniques, the Equivalent Consumption Minimization Strategy (ECMS) has received a lot of attention since it was first proposed by Paganelli in 1999 [12]. It is a static technique that relies on the instantaneous optimization of the powertrain energy flows; its theoretical bases were expanded by subsequent studies that demonstrated the correlation between the ECMS and Pontryagin's minimum principle [13]. Thus, the ECMS can generate a sub-optimal control law, but only with the a priori knowledge of the entire mission profile, because the so-called *equivalence factor* (which represents the energy conversion efficiency) must be tuned according to the driving conditions to achieve the charge sustainability. Since its initial introduction, several improvements and modifications have been proposed to direct the technique toward an online adaptation of the equivalence factor [13,14]. However, these methods do not always guarantee sub-optimal results under different driving conditions: there remains a need for calibration of the strategy.

In recent years, research on vehicular networks and communications has received a great deal of attention globally, and several car companies and government institutions are making huge investments [15]. In the frame of the Intelligent Transportation System (ITS) [16], Vehicle-to-Everything (V2X) connectivity is one of its main pillars [17]. Several papers have proved that such communications can effectively enhance safety, traffic efficiency, and energy savings, especially if coupled with Connected and Automated Vehicles (CAVs) deployment [18,19]. As a result, the connectivity level of the last-generation vehicles is continuously growing. In an HEV framework, the adoption of CAVs can lead to unprecedented results in terms of energy savings [20,21]. In particular, through V2X connectivity, the powertrain control system can gain access to relevant information on future route and traffic conditions, enabling reliable speed prediction, as demonstrated in [22]. In this framework, several works have investigated the opportunities provided by an EMS based on the ECMS in an intelligent transportation environment [23,24].

On the other hand, the sharp increase in Central Processing Unit (CPU) processing capacity, in addition to the possibility of scaling up computations on cloud platforms, has led to increasing interest in the exploitation of machine learning techniques. Many papers have proved the capabilities of Neural Networks (NNs) to solve a variety of problems [25] (e.g., pattern recognition, clustering, classification, etc.), including the energy management of HEVs [26,27,28]. In particular, if coupled with V2X connectivity, the performance of machine learning techniques can strongly benefit from information on future routes and traffic conditions. If a reliable speed prediction can be obtained from V2X connectivity, it can be considered as a sequence of data as a function of time or space, where the vehicle speed at a certain time instant is strictly correlated with both the sections preceding and following the specific value. Among the deep learning techniques, i.e., Deep Neural Networks (DNNs), Convolution Neural Networks (CNNs), and Recurrent Neural Networks (RNNs), the latter can deal with temporal information of input data, thus can capture the hidden correlations between speed values. Specifically, RNNs architecture can update the current state based on the feedback of both the current input data and the past states (the so-called "short-term memory) [29]. However, when dealing with a large gap between the relevant input data, the error signals "flowing backward in time" tend to either blow up or vanish. To overcome the error back-flow problems, and correctly handle the so-called "long-term dependency", in 1997 Hochreiter and Schmidhuber proposed the Long Short-Term Memory (LSTM) layer [30]. Since they were first introduced, LSTMs have been modified and used by many researchers for numerous purposes [31,32,33]. Among the several changes, it is worth mentioning the introduction of gate f [34], which partially solves the gradient-vanishing problem typical of RNNs by discarding or keeping the information in the cell state.

In this framework, this paper proposes an innovative Adaptive V2X connectivity-based ECMS (A-V2X-ECMS), where a limited set of future operating conditions is obtained through connectivity with the surrounding environment and is exploited by LSTM networks to provide the optimal equivalence factor, as described in Fig. 1. The novelty of this work consists of the algorithm developed for the equivalence factor selection: differently from other works, it only uses vehicle speed prediction and does not need any calibration, except for the off-line preliminary training of the machine learning models. The proposed algorithm can guarantee charge sustainability and obtain sub-optimal results in terms of fuel consumption since the LSTM network is used to capture the hidden correlations between driving patterns and the equivalence factor of the ECMS. The LSTM network was trained by assigning the optimal equivalence factors (obtained through a genetic algorithm optimization) to the training set (the observations) on a wide range of scenarios of real driving conditions. Then, the prediction of the vehicle speed obtained from V2X connectivity is used by the LSTM

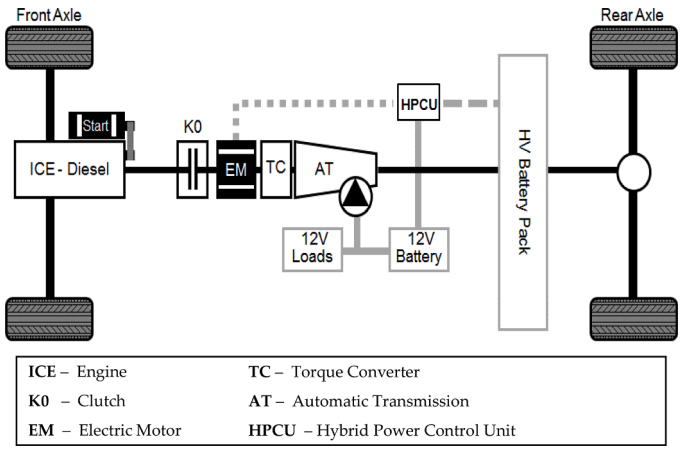

Fig. 2. Powertrain layout: it features a P2 architecture in which a diesel engine is connected through an auxiliary clutch to an EM. Both the ICE and the EM are connected to the AT through a torque converter.

Table 1
Vehicle and powertrain main specifications of the case study used in this work.

Vehicle			
Curb Weight [kg]	2060		
Power [kW] @ 100 km/h	14.9		
Configuration	Rear Wheel Drive		
Transmission			
Type	9-speed AT w/ Torque Converter		
Speed Ratios	I 5.36	IV 1.64	VII 0.87
	II 3.25	V 1.22	VIII 0.72
	III 2.26	VI 1.00	IX 0.61
Reverse	−4.93	Final Drive	2.65
Internal Combustion Engine (ICE)			
Engine Type	In-line 4 cylinders Turbo Diesel		
Displacement [cm^3]	1950		
Max Power [kW] @ 3800 rpm	143		
Max Torque [Nm] @ 1600–2800 rpm	400		
Compression Ratio	15.5:1		
Electric Machine (EM)			
Type	Permanent Magnet Synchronous motor		
Max Power [kW] @ 2000 rpm	90		
Max Torque [Nm] @ 1750 rpm	440		
Max Speed [rpm]	6000		
High Voltage Battery			
Type	Li-NMC		
Rated Voltage [V]	365		
Capacity [kWh]	13.5		
Cooling System	Water Cooled		

Table 2
Characteristic values of the cycles performed during the experimental campaign. Cycles were performed both on a chassis dynamometer and public roads.

Cycle Unit	Time [s]	Distance [km]	Avg. Speed [km/h]	Max Speed [km/h]	Avg. Acc. [m/s^2]	Max Acc. [m/s^2]	Required Energy [Wh/km]
NEDC	1180	11	34	120	0.38	1.42	184
WLTC	1800	23	47	131	0.41	1.84	222
RDE_1	4327	68	57	144	0.37	1.91	273
RDE_2	4322	68	57	128	0.36	1.74	258
RDE_3	5532	96	63	138	0.35	4.22	223
RDE_4	5926	97	59	139	0.38	3.42	225
RDE_5	6657	89	48	126	0.38	1.68	164
RDE_6	858	13	57	161	0.74	5.55	274

network to match the optimal equivalence factor to future driving conditions. The chosen value of the equivalence factor is kept constant until some trigger events occur, i.e., a radical change of driving pattern or a high deviation of the State of Charge (SoC) from the reference value. Whenever a trigger event occurs, the LSTM network is intermittently used for choosing the optimal value of the equivalence factor depending on the vehicle speed prediction. The potential of the proposed methodology in real-world conditions was assessed, through numerical simulation, on a virtual test rig of a parallel hybrid powertrain, built in [35]: the vehicle was modeled in GT-SUITE® and coupled to an EMS developed in Simulink®. The results prove that the proposed strategy guarantees charge sustainability while achieving sub-optimal results in terms of fuel consumption.

The paper is organized as follows: after presenting the main features of the case study (Section 2), the virtual test rig is described (Section 3). Then, the methodology for the definition of the A-V2X-ECMS is presented (Section 4) along with its results on the virtual test rig (Section 5).

2. Case study

2.1. Powertrain specifications

The vehicle under investigation is a state-of-the-art PHEV available in the European market. It features a P2 architecture, and the powertrain layout is schematically shown in Fig. 2. A Euro 6d-temp 1950 cc diesel engine, fitted, in a longitudinal position, at the front of the vehicle, is integrated and connected, through an auxiliary clutch (K0), to an Electric Machine (EM) of permanent magnet synchronous type. Both the ICE and the EM are connected, through a torque converter and a 9-speed Automatic Transmission (AT), to the rear axle. The EM is powered by a 13.5 kWh Li-Ion Nickel-Manganese-Cobalt-oxide (Li-NMC) High Voltage (HV) battery pack. A DC/DC converter allows the HV battery to feed the 12 V battery and all the Low Voltage (LV) loads (i.e., the 12 V starter and the electrical oil pump for gearbox lubrication). The main vehicle characteristics are summarized in Table 1.

2.2. Experimental campaign

An experimental campaign was carried out on the real vehicle, by testing it on an all-wheel drive chassis dynamometer, and in Real Driving Emissions (RDE) scenarios, equipping it with a Portable Emissions Measurement System (PEMS), as described in detail in [36].

The characteristic values of the cycles performed during the experimental campaign are shown in Table 2. As far as regulatory driving cycles (i.e., NEDC and WLTC) are concerned, measurements were performed on the chassis dynamometer following the type-approval procedure [37,38]. The Real Driving Emissions (RDE) cycles, instead, were performed to fully characterize the powertrain control logic and were conducted on public roads on the outskirts of the Italian city of Turin. As evident from Table 2, the experimental campaign allowed us to test the vehicle in a wide spectrum of driving conditions.

By way of example, the RDE_3 cycle is illustrated in Fig. 3, along with its vehicle speed and altitude profiles plotted as a function of the travelled distance. It is a pre-defined RDE-compliant route [39], and it was used as a test case for assessing the potential of the proposed methodology. In the test, a rural and a motorway operation follow the urban one, involving mild uphill and downhill sections. The total test lasted approximately 92 minutes and covered a distance of around 96 km. In Table 3, the trip composition is summarized: in an RDE-compliant cycle, each section, i.e., urban, rural, and motorway, must cover a distance higher than 16 km, while the distance share must be contained in the (23–43)% range, for the rural and motorway sections, and in the (29–44)%, for the motorway one.

2.3. Operating modes and EMS

The vehicle propulsion system, as typically for PHEVs, can operate in two different modes:

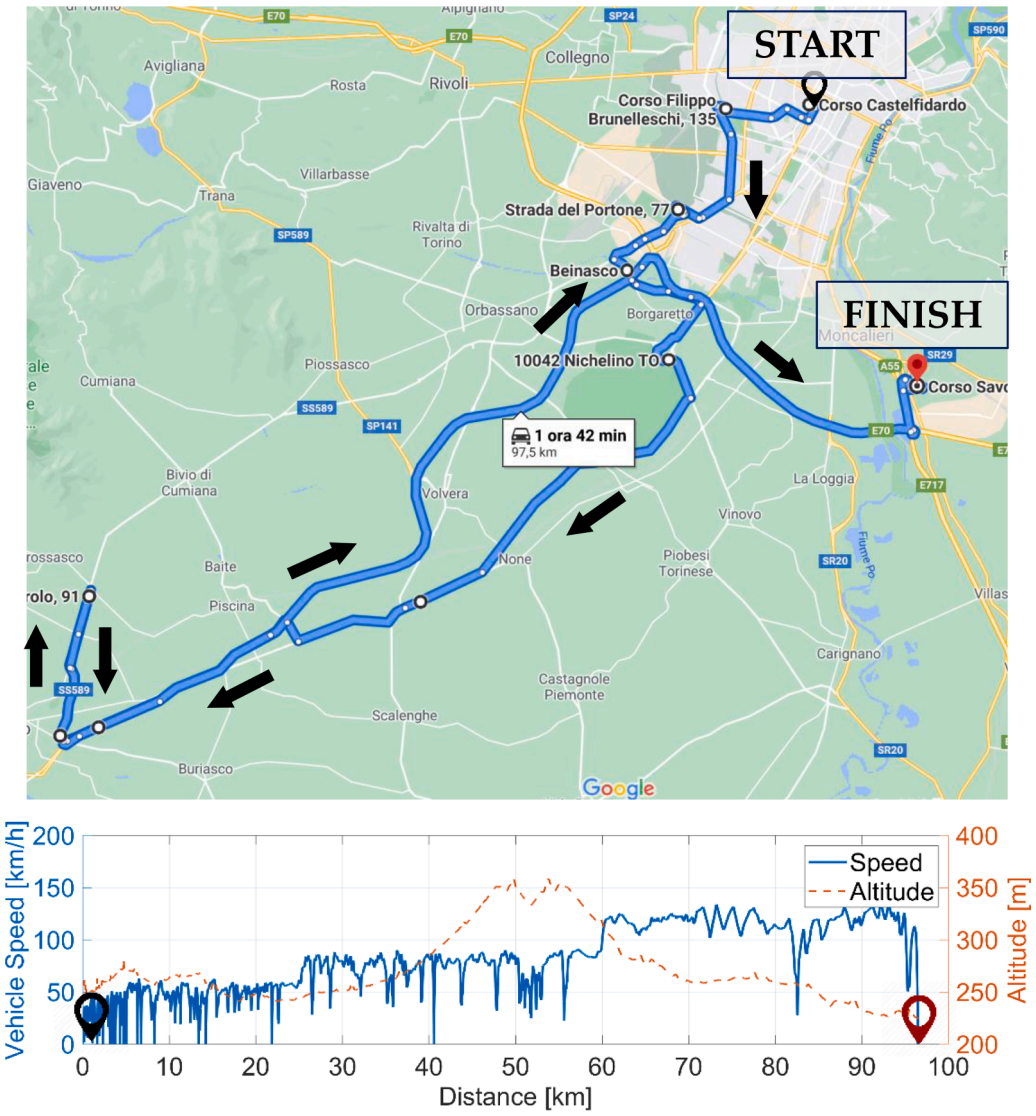

Fig. 3. RDE_3 route definition: vehicle position obtained from PEMS and combined with topographic map (Courtesy of Google Maps). The vehicle speed and altitude profiles are plotted as a function of distance.

Table 3
Trip composition of the RDE_3 cycle: the three sections, i.e., urban, rural, and motorway, are defined according to the Regulation [39].

Section Unit	Duration [s]	Distance [km]	Distance Share [%]	Average Speed [km/h]
Urban	3067	30.4	31.5	33.9
Rural	1405	31.0	32.2	76.1
Motorway	1060	35.1	36.4	113.9
Total Trip	5532	96.4	–	63.1

- Charge-Depleting (CD): when the battery is completely or partially charged, the vehicle is mainly propelled in fully electric mode;
- Charge-Sustaining (CS): when the battery SoC reaches a specific threshold defined during calibration, the ICE is mainly used for propulsion, while the EM assists the ICE to maximize its efficiency while keeping the battery SoC at an almost constant level.

The energy management strategy followed by the vehicle was extensively analyzed in [35]: without direct access to the EMS and detailed characterization of ICE, EM, and HV battery, a reverse engineering methodology was carried out to point out the dependency of the

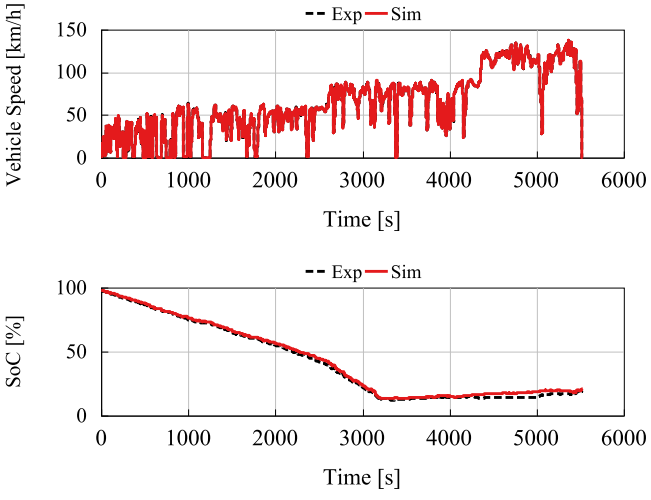

Fig. 4. Comparison between experimental data and numerical results for the speed and SoC profiles of the RDE_3.

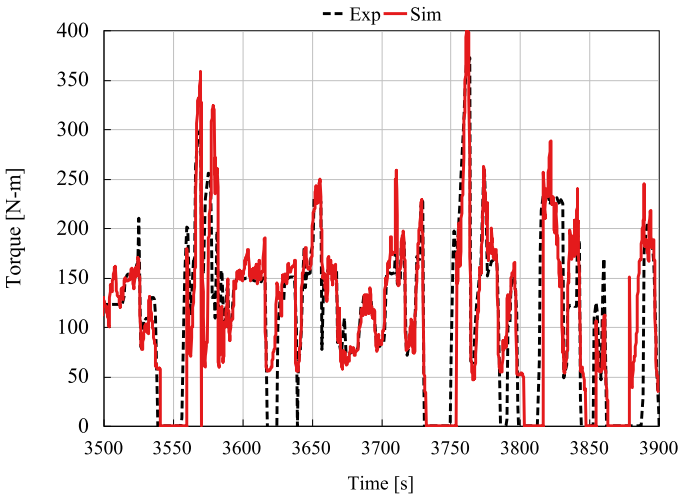

Fig. 5. Comparison between experimental and simulation results for the ICE torque on a section of the RDE_3.

Table 4
Comparison between experimental data and simulation results for the battery final SoC and the vehicle CO_2 emissions on the RDE_3.

CO_2 Specific Emissions [g/km]		Final SoC [%]	
Exp	Sim	Exp	Sim
95	96 (+1.0%)	19	18 (−4.7%)

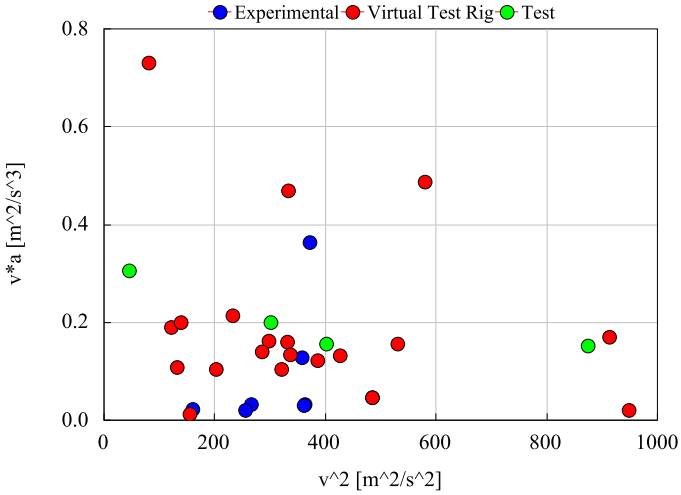

Fig. 6. Database expansion: cycles plotted as a function of squared vehicle velocity and velocity times acceleration.

EMS decisions on the powertrain main operating variables.

3. Virtual test rig

3.1. Vehicle model

In order to assess the potentialities of the advanced energy management strategy exploiting V2X information, a virtual test rig of the investigated vehicle, built in [35], was used. The model was developed in the GT-SUITE [40] software environment using a quasi-static approach [41]: a virtual vehicle driver - i.e., a Proportional–Integral–Derivative (PID) controller - compares the actual vehicle

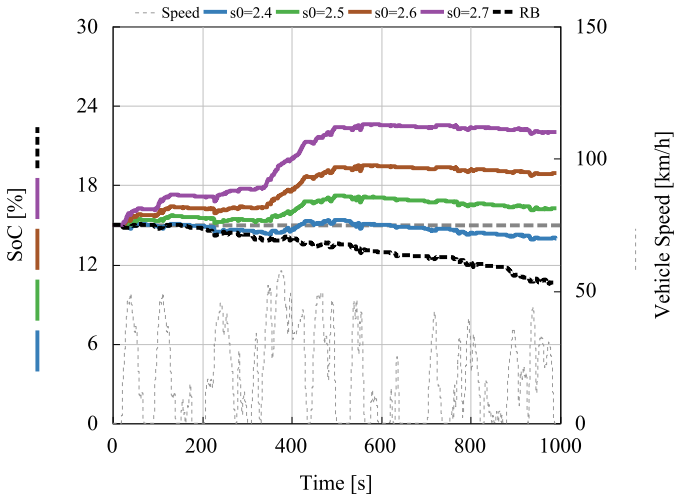

(a)

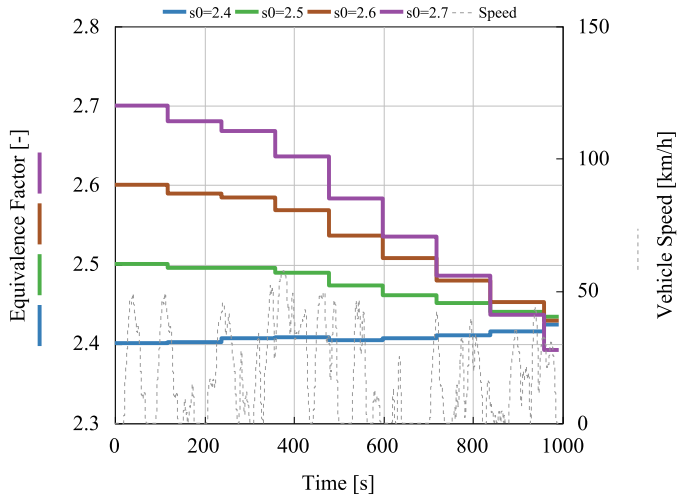

(b)

Fig. 7. The behavior of ECMS with adaptation law on the equivalence factor during the Artemis Urban cycle – (a): Battery SoC as a function of time – (b): Equivalence factor as a function of time.

Table 5
Energetic indices used as inputs to the k-means algorithm to characterize the different driving scenarios.

	Energetic Index		Unit		Energetic Index		Unit
1.	$\frac{\sum_{i=1}^{N} v_i}{N}$	$\bar{v}$	[m/s]	8.	$\frac{\int_{t_i}^{t_f} v^2(t)dt}{\int_{t_i}^{t_f} v(t)dt}$	v^2	[m/s]
2.	$std(v)$	σ_v^2	[m/s]	9.	$\frac{\int_{t_i}^{t_f} a^2(t)dt}{\int_{t_i}^{t_f} v(t)dt}$	a^2	[m/s^3]
3.	$\frac{\sum_{i=1}^{N} a_i}{N}$	$\bar{a}$	[m/s^2]	10.	$\frac{\int_{t_i}^{t_f} v(t)a(t)dt}{\int_{t_i}^{t_f} v(t)dt}$	va	[m/s^2]
4.	$std(a)$	σ_a^2	[m/s]	11.	FFT_1	P_1	[Hz]
5.	$\frac{\int_{t_i}^{t_f} v^2(t)dt}{t_f - t_i}$	I_v^2	[m^2/s^2]	12.	FFT_2	P_2	[Hz]
6.	$\frac{\int_{t_i}^{t_f} a^2(t)dt}{t_f - t_i}$	I_a^2	[m^2/s^4]	13.	FFT_3	P_3	[Hz]
7.	$\frac{\int_{t_i}^{t_f} v(t)a(t)dt}{t_f - t_i}$	I_{va}	[m^2/s^3]	14.	FFT_4	P_4	[Hz]

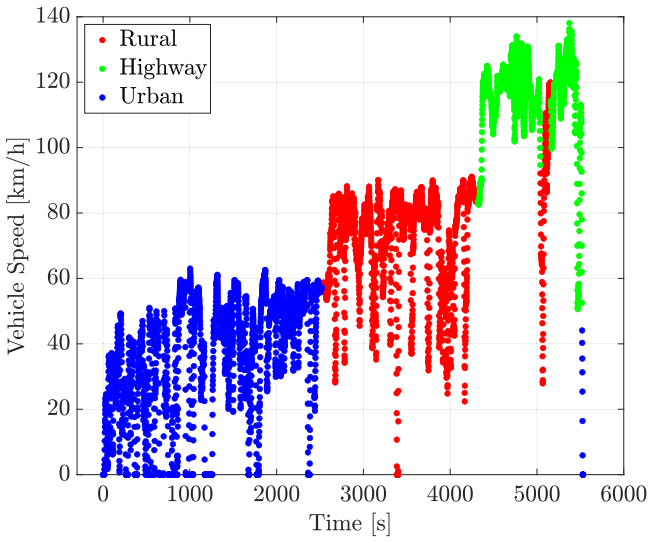

Fig. 8. Subdivisions in clusters on the RDE_3 cycle according to the k-means algorithm.

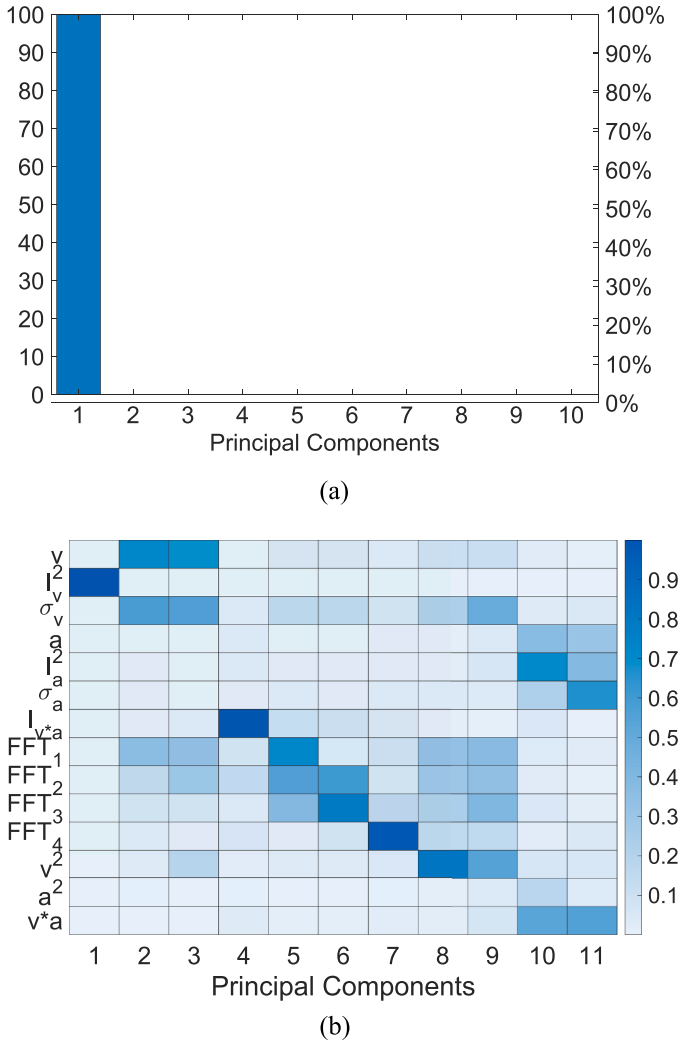

Fig. 9. PCA performed on the energetic indices. (a): Pareto chart of the principal components; (b): Heat map of the principal components - the colors represent the relative weights of the indices (the rows) for each component (the columns).

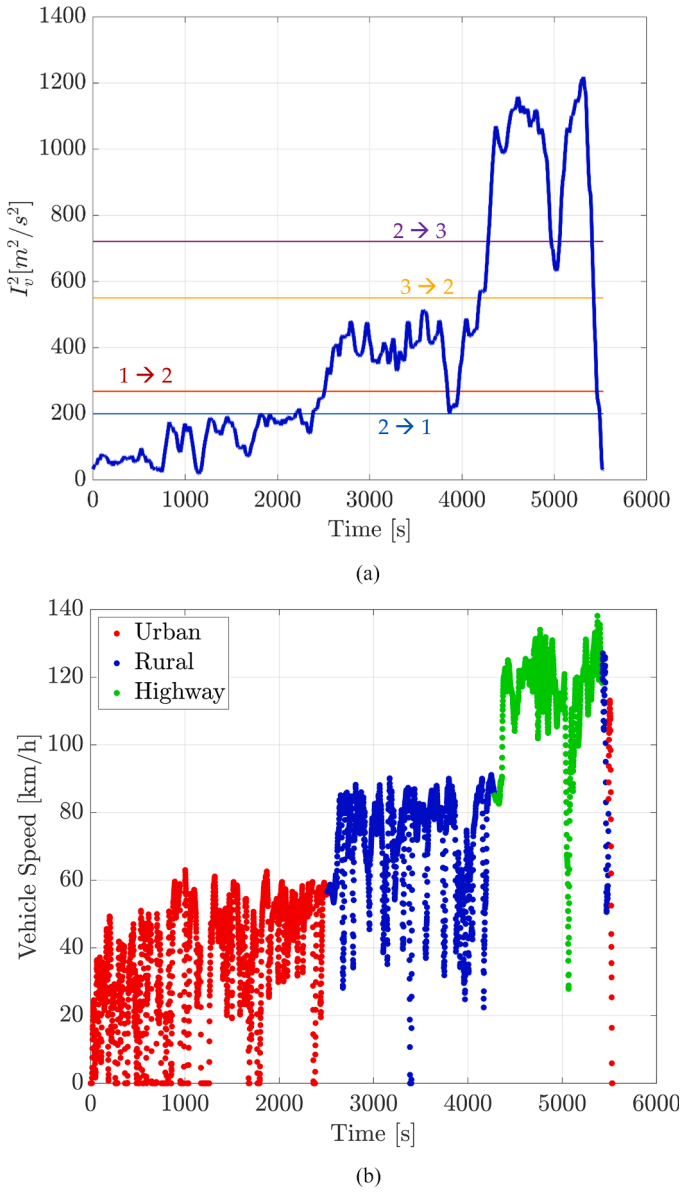

Fig. 10. (a): Index I_v^2 computed on the RDE_3 along with the defined thresholds. (b): Speed profile of the RDE_3 plotted as a function of time: the passage from one pattern to another is highlighted by a change in color.

speed to a target one and generates a power demand profile to follow the target speed. The code computes the actual vehicle speed by solving the longitudinal vehicle dynamics, while fuel consumption is calculated based on steady-state performance maps: in the literature, it has been demonstrated that steady-state maps can provide reasonable accuracy for fuel consumption estimation in driving cycles [41]. The powertrain parameters along with the performance maps were derived from [36] and are shown in Table 1.

As far as the EMS is concerned, based on the reverse engineering investigation carried out in [35], an RB control strategy was implemented in the Simulink environment and then coupled with the GT-SUITE vehicle model. The same approach (i.e., control logic developed in Simulink and coupled with the GT-SUITE model) was adopted for the ECMS control strategy. Since the proposed A-V2X-ECMS will be tested on the RDE_3 cycle, the model validation for the RB control strategy is also presented in this cycle. Fig. 4 shows the simulation results (red line) compared to the experimental measurements (black dashed line). The accurate prediction of the battery SoC trajectory - see

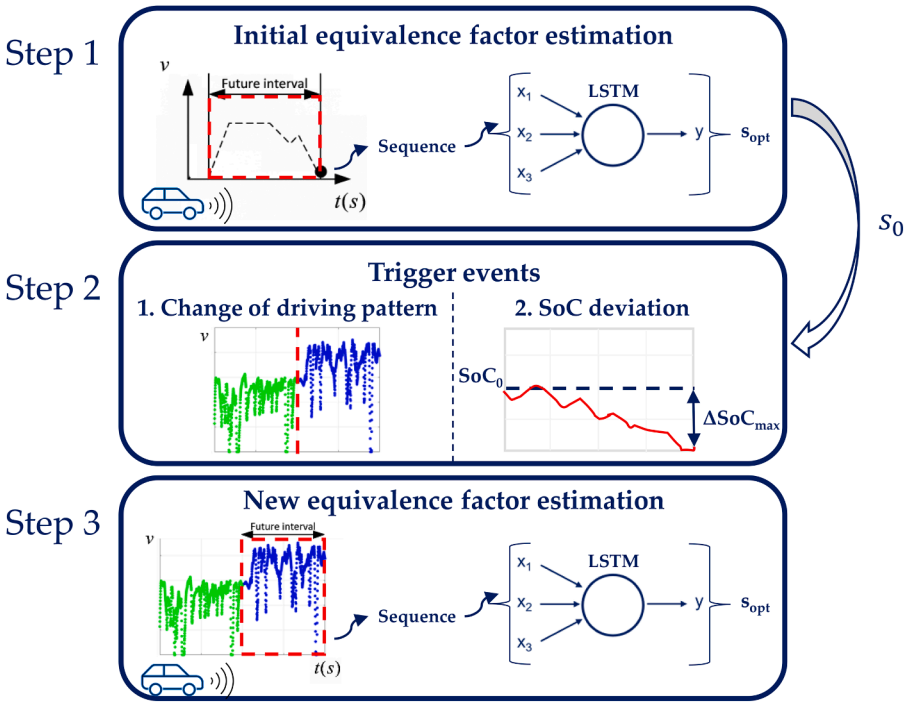

Fig. 11. The overall structure of the proposed A-V2X-ECMS methodology.

Table 6
Comparison of the computational time for different simulations featuring a standard ECMS, the proposed A-V2X-ECMS, and an A-ECMS where the equivalence factor is continuously adapted.

Computational Time	ECMS Duration	RT Factor	A-V2X-ECMS Duration	RT Factor	A-V2X-ECMS-C Duration	RT Factor
Artemis Urban	0 h 6 min 57 s	0.42	0 h 7 min 11 s	0.43	7 h 59 min 19 s	29.0
Artemis Road	0 h 8 min 10 s	0.45	0 h 8 min 1 s	0.44	8 h 40 min 4 s	28.8
Artemis Motorway	0 h 7 min 25 s	0.42	0 h 7 min 52 s	0.44	8 h 32 min 17 s	28.8

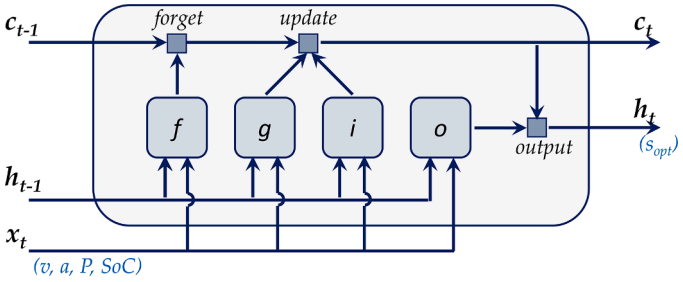

Fig. 12. LSTM layer layout: the predicted output patterns (the optimal equivalence factors) are assigned to the training set (the observations).

Table 7
Hyperparameters of the LSTM network used in the A-V2X-ECMS strategy.

Hyperparameters	Value
Number of Hidden Layers	2
nNodes1	40
nNodes2	28
Dropout	0.5418
Learn Rate	0.001
Regularization Factor	1.0620e-9

Fig. 4- and the good agreement between simulated and measured engine torque (Fig. 5) prove the robustness of the EMS obtained from the reverse engineering of the real control strategy. Furthermore, the limited errors in both the battery final SoC and the vehicle CO_2 emissions prove the reliability of the vehicle model (see Table 4). Although the discrepancy in terms of final SoC may appear quite significant (4.7%), it is quite limited if compared with the energy required on the entire driving cycle: i.e., less than 0.1 kWh over a total energy request of 21.6 kWh (0.44%). Hereinafter, the extracted control logic will be indicated as RB and will be used as a reference for the assessment of the A-ECMS performance.

3.2. Database expansion

Since the experimental tests performed on the real vehicle were limited due to time and money constraints, the experimental data would not have been sufficient to properly train the NNs. Therefore, a database expansion was performed to cover a wider spectrum of driving patterns: the virtual test rig, obtained from the model validation, was used to perform additional driving cycles in a simulated environment. The mission profiles included traces available from experimental tests performed with other vehicles and type-approval procedures available from the literature (i.e., EPA tests [42] - such as US06, FTP, etc., - Artemis cycles [43], and RTS95 [44]). The database expansion allowed us to increase the time of vehicle testing from 510 min (real vehicle) to 1927 min (real vehicle + virtual tests). Fig. 6 displays all the cycles as a function of two main energetic indices: the square of the average vehicle

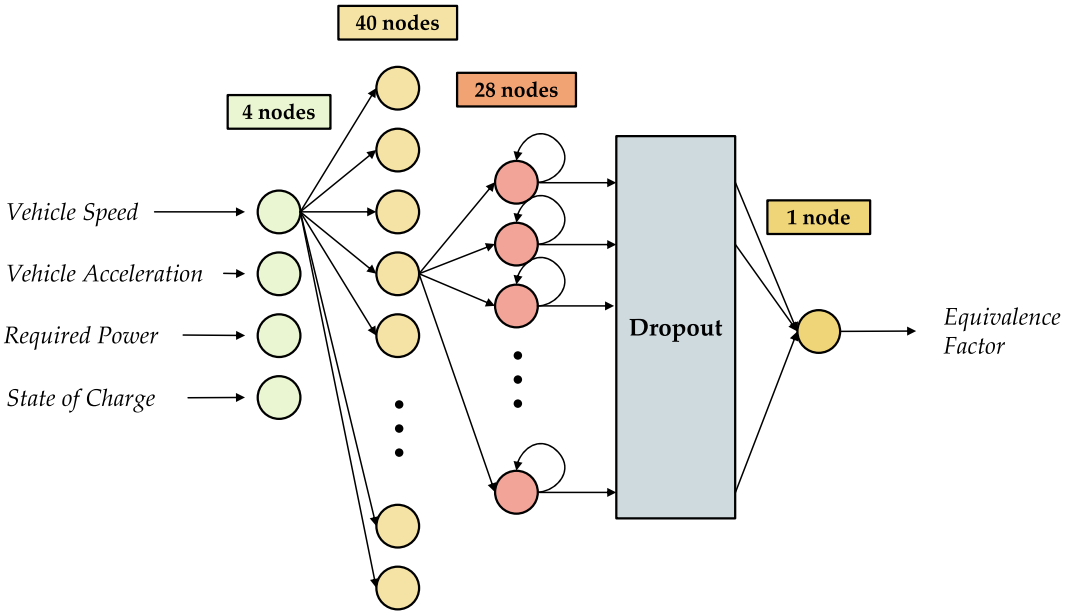

Fig. 13. Topology of the LSTM network: inputs layer, 2 fully connected layers, dropout layer, and regression output layer.

velocity, on the x-axis, is related to the average energy required in a cycle, while the product of average vehicle velocity and average vehicle acceleration is an indicator of the driving cycle aggressiveness. It is quite evident that the database expansion allowed us to increase the area covered by the experimental tests (only blue dots). It is worth noting that the cycles selected for testing the proposed strategy (green dots) are well distributed over the plot.

4. Enhancing EMS: A-V2X-ECMS

Since the experimental investigation highlighted the typical operating modes of a PHEV (i.e., CD followed by CS), the methodology proposed by this paper was primarily developed for CS operations. The results of the proposed methodology will be compared with the following strategies:

- RB:

This strategy was extracted from the experimental campaign carried out on the real vehicle: it employs simple rules, thus making it easily implementable in a vehicle Electronic Control Unit (ECU). However, it is highly sensitive to any change, in driving conditions, from the ones used for calibration.

- Optimal ECMS:

This strategy can obtain optimal results, but it requires the a-priori knowledge of the entire vehicle speed profile. Since it is not feasible in real-world scenarios, it was used as a reference for optimal results. The equivalence factor, used in the simulations, was obtained through a genetic algorithm optimization.

- Reference A-ECMS:

This strategy was introduced to adapt the equivalence factor in real-world scenarios, according to the varying conditions. However, the adaptation law must be properly calibrated according to the driving conditions.

The strategy proposed in this work is:

- A-V2X-ECMS:

This strategy can improve the performance of a standard adaptation algorithm by introducing information about future vehicle driving patterns. In this work, V2X connectivity is assumed to provide a reliable speed prediction.

4.1. Energy management problem

4.1.1. ECMS

The optimal control problem of an HEV can be addressed with several methods [45]; in this paper, the authors decided to implement a local optimization strategy, i.e., the ECMS, thanks to its potential to achieve sub-optimal results, while being feasible in a vehicle ECU. The basic idea of the ECMS is to move from a global optimization problem to a local minimization one: an equivalent fuel consumption, obtained by summing the actual engine fuel consumption, $\dot{m}_f(t)$, to an equivalent fuel consumption related to the use of the battery, $\dot{m}_{el}(t)$, is minimized at each instant of time [12]:

$$\dot{m}_{f,eq}(t) = \dot{m}_f(t) + \dot{m}_{el}(t) = \dot{m}_f(t) + \frac{s(t)\cdot P_{batt}(t)}{Q_{LHV}} \quad (1)$$

Where $P_{batt}(t)$ is the instantaneous power provided ($P_{batt}>0$) or absorbed ($P_{batt}<0$) by the battery; Q_{LHV} [MJ/kg] is the fuel lower heating value (energy content per unit of mass); $s(t)$ is the instantaneous equivalence factor converting the battery energy consumption into a corresponding (or "equivalent") fuel consumption; P_{batt} is the control variable and can range from minimum to maximum admissible values. However, this approach requires the appropriate value of equivalence factor $s(t)$ to properly estimate the cost of the energy stored in the battery: its optimal value, which entails the SoC balance at the end of the cycle, depends on both the main features of the powertrain and the specific mission profile. A wrong guessing of this parameter may jeopardize the benefits of the ECMS leading to results far from optimality.

4.1.2. Reference A-ECMS

In real-world conditions, where driving patterns are neither repetitive nor completely predictable, the equivalence factor must be adapted online to provide robustness and, ideally, obtain results close to the optimum. The most common methodology for the adaptation of the equivalence factor relies on a mathematical expression, which periodically modifies this parameter based on its past values and the difference

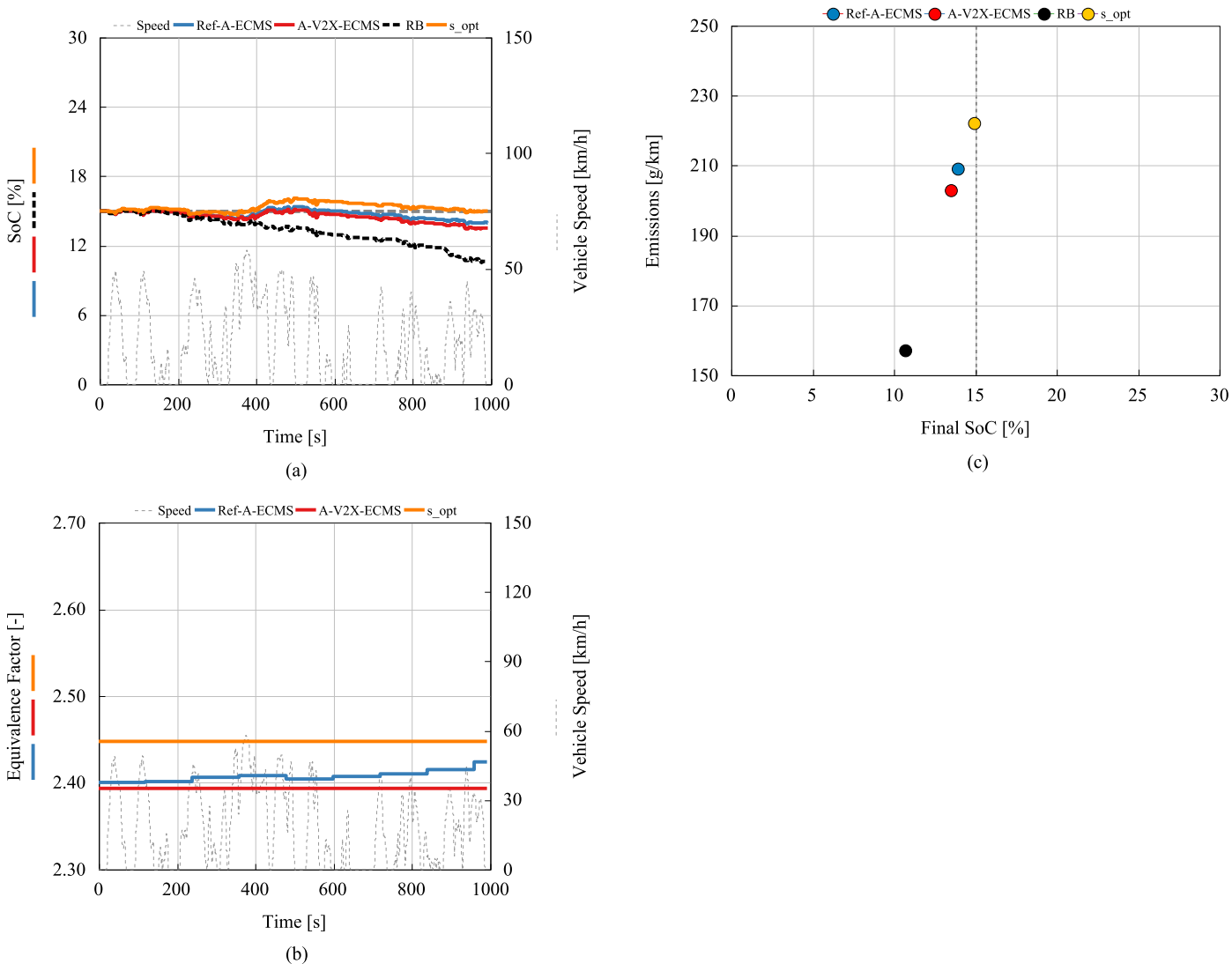

Fig. 14. Comparison of the results over the Artemis Urban cycle for RB, Ref. A-ECMS, A-V2X-ECMS, and ECMS optimized for CS conditions – (a): SoC as a function of time – (b): Equivalence factor as a function of time – (c): Tradeoff between CO_2 emissions and final SoC.

between actual and reference SoC [14]:

$$s_{k+1} = \frac{1}{2}(s_k + s_{k-1}) + k_p(SoC_0 - SoC(t))$$
$$t = kT,\ k = 1, 2, \ldots \tag{2}$$

Where s_k is the value of the equivalence factor currently used; s_{k-1} is the value used in the previous time interval; s_{k+1} is the value that will be used in the subsequent time interval; $(SoC_0\text{-}SoC(t))$ is the difference between reference and actual SoC values, at the instant of the adaptation; k_p is the proportional gain of the feedback controller; T is the adaptation period. It should be noted that since the strategy aims to achieve charge sustainability, the initial SoC is used as the reference value. Based on some preliminary analyses omitted, for the sake of brevity, in this context, k_p is imposed equal to 1, while, coherently with [14], a compromise value was chosen for the period of adaptation T, i.e., $T = 120$ s.

By way of example, the adaptation law introduced in [14] was tested over the Artemis Urban cycle [43]. The sensitivity analysis reported in Fig. 7, where the SoC trend is plotted for an ECMS with four different initial equivalence factors, ranging from 2.4 to 2.7, demonstrates that this formula guarantees a reactive correction of the equivalence factor - see Fig. 7(b) - but, if wrongly initialized, it may not achieve the CS condition (see, for instance, the case with s_0=2.7). Moreover, since this formula does not use any information about the future driving conditions of the vehicle, if they change significantly, the algorithm will react only at the end of the adaptation period, compensating for the deviation of the SoC from the reference value.

Hereinafter, this strategy will be referred to as Ref. A-ECMS, and, when used as a benchmark, a trade-off value will be used for the initial equivalence factor s_0.

4.2. Methodology proposed: A-V2X-ECMS

4.2.1. Driving pattern recognition

For a given vehicle configuration, the characteristics of a certain driving scenario can be directly related to the energy required by the powertrain, which strongly affects its efficiency. Since the equivalence factor represents the efficiency of the powertrain energy flows, it is possible to find a correlation between its optimal value and the driving conditions. To achieve this goal, it is essential to identify one or more energetic indices that can fully characterize a certain driving scenario. In this work, an unsupervised learning technique [46] was employed to identify similar patterns in the analyzed data. The number of clusters was chosen according to the typical classification used in the EU Regulation [39]: urban, rural, and highway. Starting from the expanded

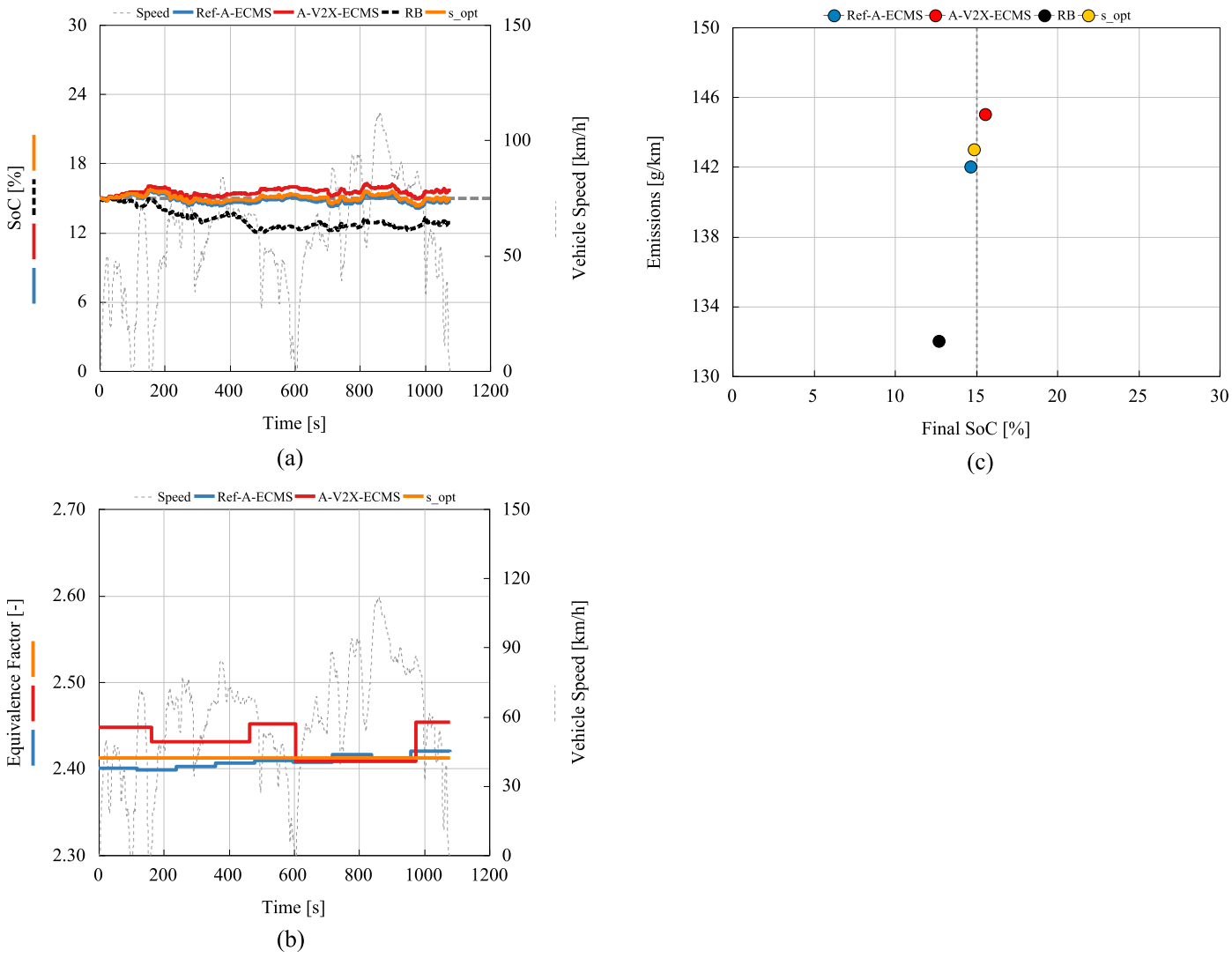

Fig. 15. Comparison of the results over the Artemis Road cycle for RB, Ref. A-ECMS, A-V2X-ECMS, and ECMS optimized for charge sustaining conditions – (a): SoC as a function of time – (b): Equivalence factor as a function of time – (c): Tradeoff between CO_2 emissions and final SoC.

database, described in Section 3.2, each mission profile was subdivided into sub-cycles, lasting 120 s each: the time interval is a tradeoff value between the requirements of a reliable speed prediction and a sufficiently long interval to contain significant information. Several energetic indices, listed in Table 5, were chosen for collecting information about the driving patterns of each sub-cycle and used as inputs for the unsupervised learning technique. The indices were defined by applying simple statistical formulas to the vehicle speed and acceleration, while the Fast Fourier Transform (FFT) algorithm was used to compute the first four harmonics of the velocity signal (*FFTs* in Table 5). Specifically, $v(t)$ is the vehicle speed, $a(t)$ is the vehicle acceleration, t_f is the final time, t_i is the initial time, and N is the number of sampling points. The k-means algorithm [47] was chosen for this application: this technique initially chooses k arbitrary centers (i.e., values of the energetic indices) and assigns each point (energetic indices calculated on each sub-cycle) to the nearest center; then, each center is recomputed as the center of mass of all points assigned to it. These two steps (assignment and center calculation) are repeated until the process converges to a stable solution. The main advantage of this algorithm lies in its speed since very few iterations are usually required to reach convergence.

In Fig. 8 the clusters identified by the k-means algorithm are shown for the RDE_3 cycle: this technique can correctly recognize the different driving patterns. The first portion of the driving cycle, which is conducted within the city of Turin, is identified as the first cluster (which we called *urban*); while the second part of the driving cycle, which occurred in extra-urban driving conditions, is subdivided into the other two clusters (namely *rural* and *highway*). Similar results were obtained for the other mission profiles proving that the k-means algorithm can provide satisfying performance in driving pattern recognition.

The next step consisted in reducing the number of indices through a Principal Component Analysis (PCA) [48], which, by performing a linear transformation, detects most of the variance with the first few principal components. As evident from the Pareto chart in Fig. 9(a), the first principal component can virtually describe all the variability among the data set (the bars represent the corresponding weight of each principal component), while, the heat map, depicted in Fig. 9(b), shows that the first principal component is mainly composed by the energetic index I_v^2 (#5 in Table 5) – the colors represent the relative weights of the indices (the rows) for each component (the columns). The PCA suggests that a k-means algorithm, based only on the I_v^2 index, can correctly assign each sub-cycle to the corresponding cluster. Hence, only the index I_v^2 will be used for driving pattern recognition.

The last step consisted in obtaining a strategy that could be implemented online. Since the k-means algorithm can only provide a posteriori driving pattern identification, a different approach was required to obtain a real-time correction of the equivalence factor. Thus, some

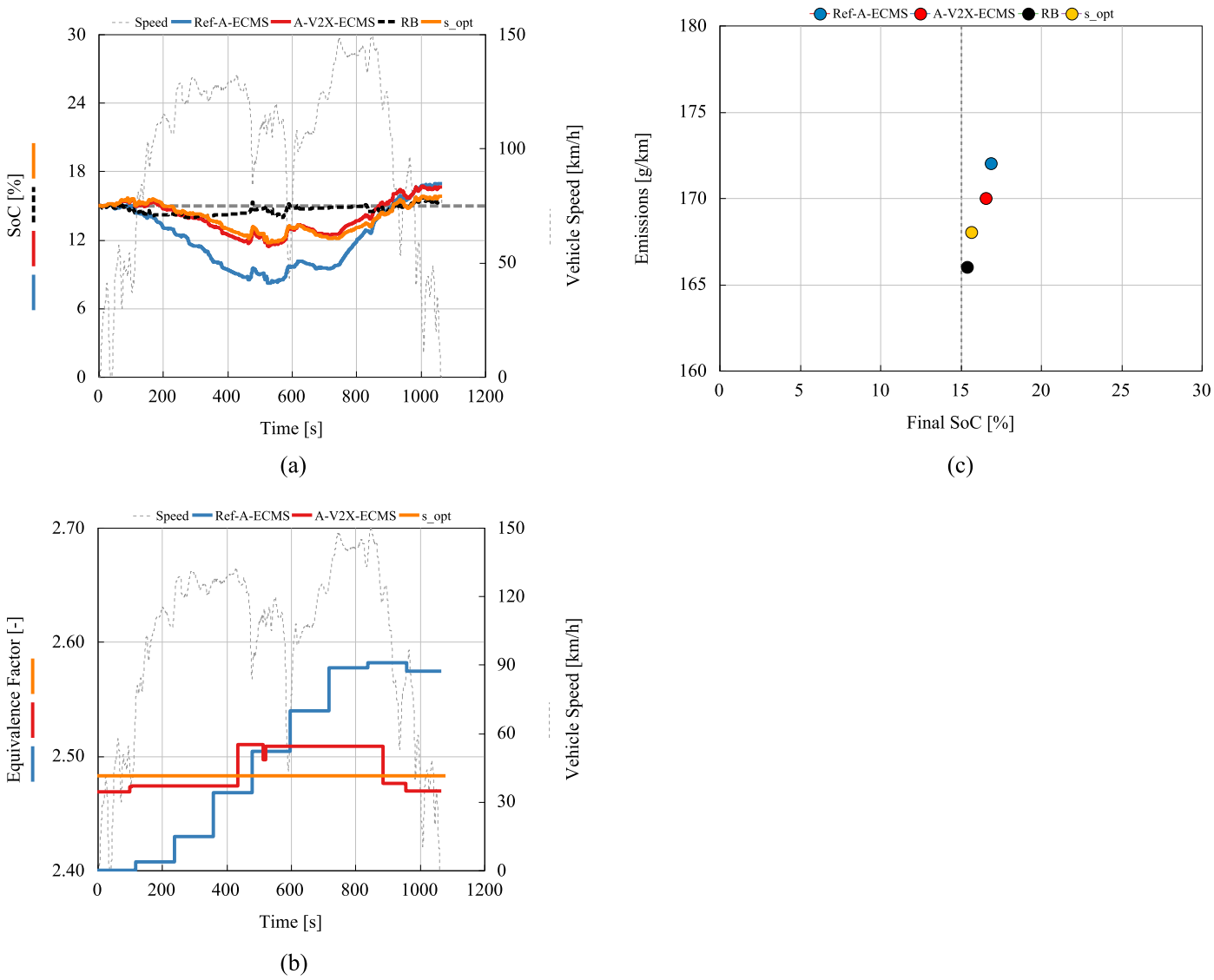

Fig. 16. Comparison of the results over the Artemis Motorway cycle for RB, Ref. A-ECMS, A-V2X-ECMS, and ECMS optimized for CS conditions – (a): SoC as a function of time – (b): Equivalence factor as a function of time – (c): Tradeoff between CO_2 emissions and final SoC.

threshold levels of the I_v^2 index were identified from the entire dataset: all the values, determining a transition from one cluster to another, were collected and used for computing the average values. Coherently with the time interval used in the k-means algorithm, we chose to compute this index over an interval of 120 s. Fig. 10(a) shows the profile of the I_v^2 index along with the identified threshold values, while, in Fig. 10(b), the passage from one pattern to another is highlighted by a change in color. The threshold levels regulate the transitions from one cluster to another (i.e., 1→2 from urban to rural and vice versa 2→1; 2→3 from rural to highway and vice versa 3→2). The I_v^2 index is computed by assuming the knowledge of the future vehicle speed: specifically, the integration range is a 120 s window starting from the specific point (see the formula in Table 5). Comparing Figs. 8 and 10(b), it is clear that the thresholds of the I_v^2 index can achieve an online cluster identification consistent with the one obtained a posteriori by the k-means algorithm. Similar results were obtained for all the other cycles on which the I_v^2 index was tested.

4.2.2. A-V2X-ECMS

Several car manufacturers are already using Global Positioning System (GPS) information in the energy management of HEVs in order to better exploit the electrification potentialities. For the vehicle under analysis, the authors in [35] demonstrated that, when provided with information through the navigation system, the EMS behaves differently by adjusting the control law depending on the driving pattern. In this context, V2X information could likely be shortly integrated into the control logic of a vehicle. While the limits of a strategy only relying on past information have already been outlined in Section 4.1, an adaptation algorithm exploiting information from V2X connectivity may be able to avoid undesired oscillations of the equivalence factor and achieve a control strategy closer to optimality. This section aims to describe a methodology capable of improving the performance of a standard adaptation algorithm by introducing information about future vehicle driving patterns, where V2X connectivity is assumed to provide a reliable speed prediction. Since this work represents a preliminary assessment of the algorithm potentiality, a perfect knowledge of the future speed profile is assumed (e.g., the uncertainties related to the estimation of traffic conditions are neglected).

The overall structure of the proposed methodology is shown in Fig. 11. Differently from the standard formulation, the initial value of the equivalence factor is provided by an LSTM network, that was trained for assigning the optimal value of the equivalence factor to the future driving conditions (see Section 4.2.3) depending on the current SoC level. Then, the value of the equivalence factor is kept constant until a trigger event occurs, i.e., a radical change of driving pattern (e.g., a

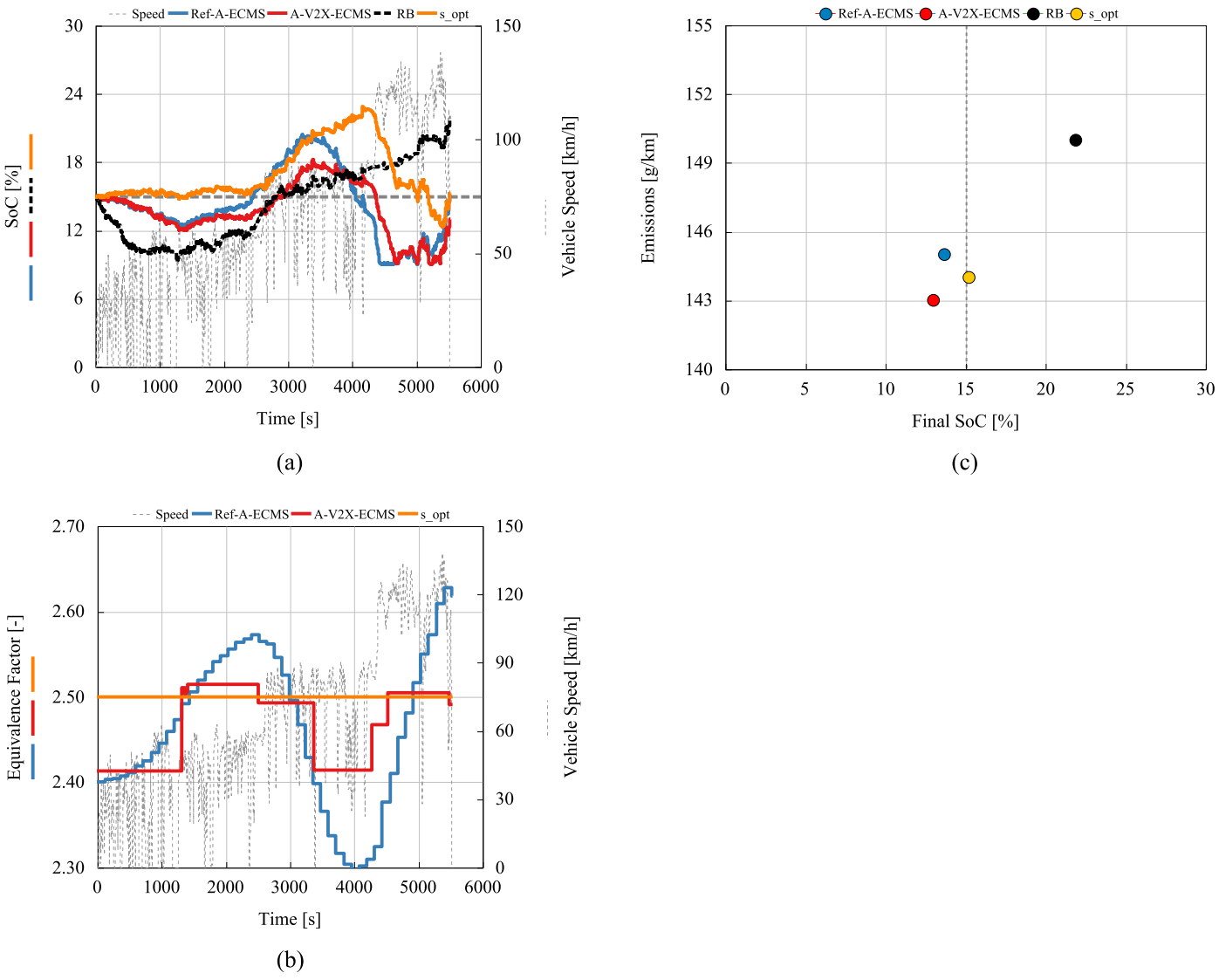

Fig. 17. Comparison of the results over the RDE_3 cycle for RB, Ref. A-ECMS, A-V2X-ECMS, and ECMS optimized for CS conditions – (a): SoC as a function of time – (b): Equivalence factor as a function of time – (c): Tradeoff between CO_2 emissions and final SoC.

vehicle moving from urban areas to the highway) or a high deviation of the SoC from the reference value. As far as the change in the driving pattern is concerned, the energetic index I_v^2 is used to report it. Then, the LSTM network is used to choose a new optimized value of equivalence factor depending on the vehicle speed prediction and actual SoC level. By comparing this methodology to the standard law proposed in [14], proactive behavior is introduced by employing information deriving from V2X connectivity.

It should be noted that the proposed methodology does not excessively increase the computational time if compared to a standard ECMS. Although the NNs require additional computational effort to compute the optimal equivalence factor, this computation is performed only at the beginning of the route or when a trigger event occurs. Table 6 displays the computational time required for performing the simulations along with the Real-Time (RT) factor, i.e., the ratio between simulation and real-life cycle duration. It is evident that, in all the simulations, the RT factors of the proposed A-V2X-ECMS are quite close to the ECMS ones, making this strategy feasible in a vehicle ECU. On the contrary, if the NNs are continuously used for updating the equivalence factor (see A-V2X-ECMS-C), the computational time drastically increases, leading to a non-feasible strategy. The computational times here shown refer to a PC with the following specifications: Intel (R) Core (TM) i7–2600 CPU @ 3.40 GHz, 3.40 GHz, 16 GB RAM.

It should be noticed that the training phase of the LSTM network is not considered in Table 6. This phase requires high computational times, however, it is carried out offline, while, in terms of feasibility, only the computations performed online should be considered. Section 4.2.3 will describe the procedure followed for training the LSTM network in assigning the optimal equivalence factor to a specific driving cycle.

4.2.3. *LSTM deep neural networks training*

Fig. 12 shows a schematic of the standard LSTM cell. x_t is the input at time step t, c_t is the cell state, containing information from the previous time steps and h_t is the output state (also known as the hidden state). W are the input weights, R are the recurrent weights, and b are the bias; i, f, and o, denote input, forget, and output gate, respectively, while g denotes the cell candidate. At time step t, the block uses the current state of the network (c_{t-1}, h_{t-1}) and the following input of the sequence to compute the output and update the cell state c_t. The layer adds or removes information from the cell state through the gates: gate f, for example, is in charge of deciding what information must be kept or discarded. Based on the connections shown in Fig. 12, the LSTM cell can be mathematically expressed as in Eq. (3):

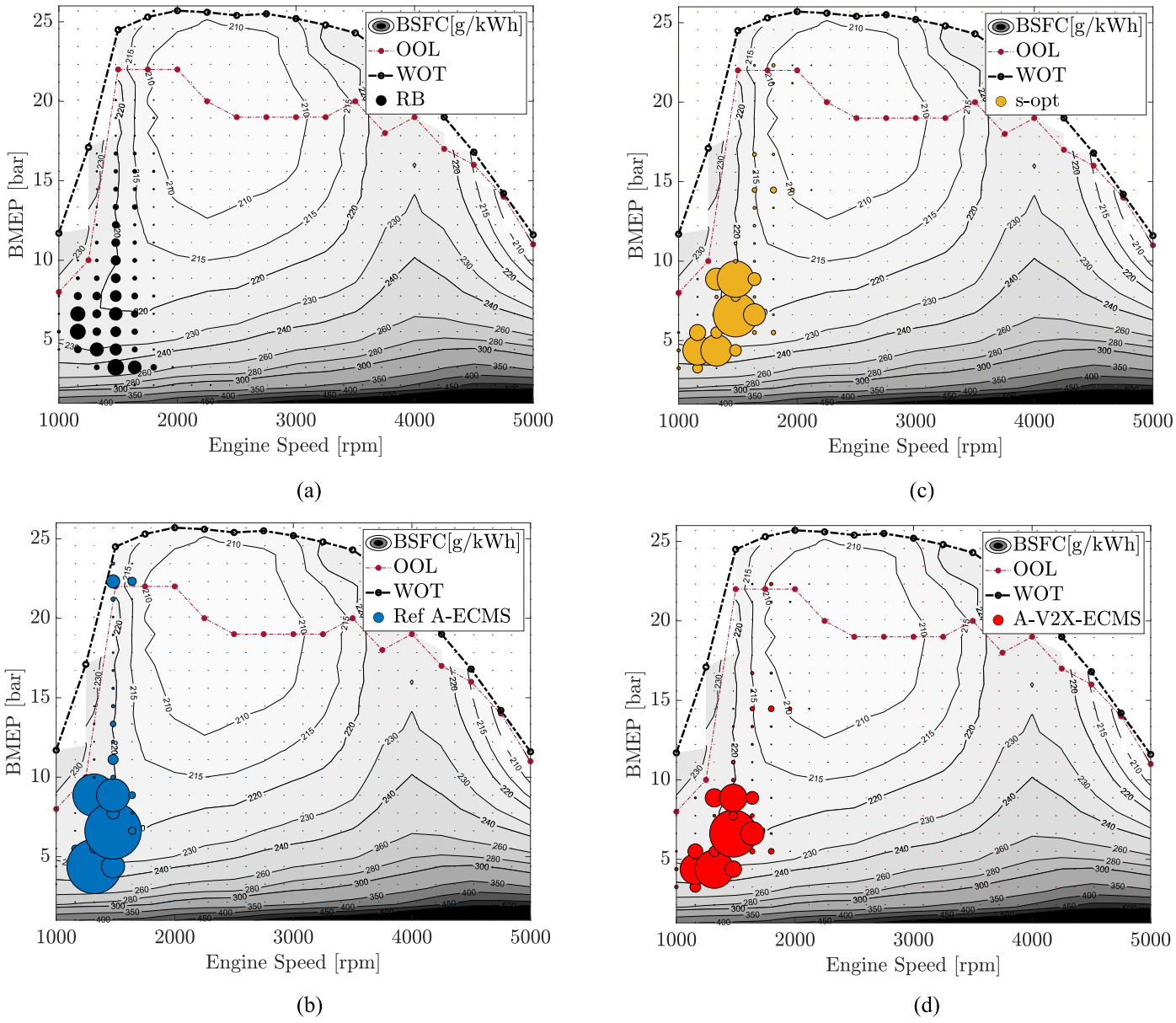

Fig. 18. Comparison of the ICE operating points over the RDE_3 cycle reported on the BSFC map – (a): RB – (b): opt. ECMS – (c): Ref. A-ECMS – (d): A-VX-ECMS.

$$
\begin{aligned}
i_t &= \sigma_g(W_i x_t + R_i h_{t-1} + b_i) \\
f_t &= \sigma_g(W_f x_t + R_f h_{t-1} + b_f) \\
g_t &= \sigma_c(W_g x_t + R_g h_{t-1} + b_g) \\
o_t &= \sigma_g(W_o x_t + R_o h_{t-1} + b_o) \\
c_t &= f_t \cdot c_{t-1} + i_t \cdot g_t \\
h_t &= o_t \cdot \sigma_c(c_t)
\end{aligned}
\tag{3}
$$

The training session was performed with the same database used for the k-means algorithm. However, for this analysis, the 32 mission profiles were subdivided into sub-cycles of various lengths assigned to urban, rural, and highway clusters. For each sub-cycle, 7 different levels of initial SoC were analyzed from 0.1 to 0.25. Each sub-cycle was considered as an observation: a set of sequences, i.e., the vehicle speed, the vehicle acceleration, the power required, and the initial SoC. Considering all the sub-cycles and the corresponding SoC levels, 1169 observations were available. The SoC was added to account for the excess or deficit of energy associated with the difference between the actual and the target SoC values. This allowed the LSTM network to correctly choose the optimal equivalence factor also in case of major discrepancies between actual and target SoC values.

At the same time, using the virtual test rig validated in the early stages of the project, the optimal equivalence factor was computed for all the sub-cycles at the different initial SoC levels, through a genetic algorithm optimization aimed at achieving the target final SoC. The optimal equivalence factor was allowed to vary in the range between 1.5 and 3.0. All the cases featuring a boundary value were discarded since they were considered not significant for the analysis: i.e., the SoC target could not be reached due to the excessive difference between the initial and final SoC. This screening led from the initial 1169 observations to 944 ones used in the training phase. Then, the LSTM network was trained by assigning the predicted output patterns (the optimal equivalence factors) to the training set (the observations), as shown in Fig. 12.

The experiment manager app [49] was used for the definition of the hyperparameters of the network, i.e., all the fixed parameters chosen by the user and not tuned during the training phase. This tool allows the training of networks under multiple initial conditions, where the hyperparameters can vary in a range defined by the user. Concerning the LSTM network used in this paper, the values of the hyperparameters, shown in Table 7, were obtained through Bayesian optimization. The

topology of the LSTM network is shown in Fig. 13: the network starts with an input layer, featuring 4 sequences (i.e., vehicle speed, vehicle acceleration, required power, and initial SoC); then it has two fully connected layers with 40 and 28 nodes, respectively. Finally, it ends with a dropout layer and a regression output layer.

5. Results

In this section, the results of the proposed A-V2X-ECMS are compared with Ref. A-ECMS (where a tradeoff initial value is chosen for the equivalence factor), the RB strategy (extracted from the experimental campaign on the real vehicle), and the ECMS featuring the optimal equivalence factor (employing a genetic algorithm optimization over the entire a priori known vehicle mission profile to achieve the target final SoC). As already mentioned, the simulations are carried out only in CS conditions. The fuel economy potential of the A-V2X-ECMS is preliminarily assessed on the Artemis driving cycles [43] since they closely mimic real-world driving conditions. Moreover, since the Artemis driving cycles include three distinct cycles, the potential of the proposed strategy can be evaluated separately under each driving scenario, i.e., urban, rural, and motorway. Afterward, the proposed A-V2X-ECMS is tested over the RDE_3 cycle to prove its capabilities in a driving scenario that follows all the requirements of the RDE Regulation [39]. It is worth mentioning that the cycles used for testing the LSTM network were not used during the training phase.

5.1. Artemis driving cycle

In Fig. 14(a), the SoC trend of the A-V2X-ECMS is compared with the RB logic, the Ref. A-ECMS, and the ECMS featuring the optimal equivalence factor, while in Fig. 14(b) the trends of the equivalence factor are plotted as a function of time. Finally, in Fig. 14(c), the tradeoff between CO_2 emissions and final SoC is represented for all four cases. As it can be easily seen, the RB strategy is the one obtaining the lower CO_2 emissions. However, the final SoC is quite far from the target value. Instead, both the Ref. A-ECMS and the A-V2X-ECMS can guarantee the CS condition while having CO_2 emissions not far from the optimal ECMS. As illustrated by Fig. 14(b), the equivalence factor of the Ref. A-ECMS is periodically updated according to [14], depending on the difference between actual and reference SoC. Instead, in the A-V2X-ECMS, since no trigger event occurs in this cycle (i.e., no radical change of driving pattern and no high deviation of the SoC from the reference value), the equivalence factor is kept constant over the entire driving cycle. The initial guess of the LSTM network is not so far from the optimal value of equivalence factor – 2% of error.

In Fig. 15, the same plots are reported for the Artemis Road cycle: it can be observed that the RB strategy obtains the lower CO_2 emissions at the expense of an extremely low final SoC. The A-V2X-ECMS performance is not so far from both the optimal ECMS and the Ref. A-ECMS. Since trigger events occur in this cycle (i.e., the passage from urban to rural driving conditions and vice versa), the equivalence factor is repeatedly updated, and the LSTM network tunes its value according to the future driving conditions.

In Fig. 16, the same plots are reported for the Artemis Motorway. In this cycle, all four strategies reach charge sustainability and the results in terms of the tradeoff between CO_2 emissions and final SoC values are comparable. As evident from Fig. 16(a) and (b), Ref. A-ECMS causes a significant deviation of the SoC from the target value, leading to big corrections of the equivalence factor. On the other hand, in the A-V2X-ECMS, the assignment of the equivalence factor to each section of the driving cycle limits its variation in a range much closer to the optimal one. This leads to a smaller excursion of the SoC during the cycle, if compared to Ref. A-ECMS.

5.2. Real driving emission test

In this section, the results of the A-V2X-ECMS are compared with the RB logic, the Ref. A-ECMS, and the ECMS featuring the optimal equivalence factor, over the RDE_3 cycle, to prove its capabilities in a real-driving scenario. Regarding the RB strategy, it should be noted that, while the model validation was performed in CD+CS operation (see Fig. 4), in this section the RB strategy is simulated only in CS operation. As evident from Fig. 17(b), the RB strategy is not able to achieve charge sustainability. In fact, by excessively using the ICE to charge the battery, it is not able to fully exploit the hybrid powertrain potential, leading to higher CO_2 emissions. On the contrary, the A-V2X ECMS is able to reach a final SoC value not so far from the optimal ECMS, and the Ref. A-ECMS. Moreover, by looking at Fig. 17(b), it is quite evident that the A-V2X-ECMS allows a strong decrease in the oscillations of the equivalence factor and, consequently, in the SoC swings if compared to the Ref. A-ECMS formulation. In terms of charge sustainability, the two methodologies are quite comparable (see Fig. 17(c)), but by considering the entire mission profile, for the A-V2X-ECMS the SoC is confined in a smaller interval around the target value, thus leading to a better tradeoff between CO_2 emissions and final SoC. The A-V2X-ECMS updates the equivalence factor only when a change in the driving pattern occurs or a deviation from the SoC target is detected: the strategy chooses the most appropriate equivalence factor for each section, and achieves better performance, in terms of fuel economy, over the entire cycle.

The differences between the four strategies, in terms of engine operation optimization, can be seen in Fig. 18, where the ICE working points over the RDE_3 are plotted on its Brake Specific Fuel Consumption (BSFC) map. The engine operating points are represented by circle markers whose size is proportional to the time spent by the engine in that region. Comparing Fig. 18(a) with all the others, it is evident that, when the power split is decided by the RB strategy, the ICE is operated in a wider area; instead, when the power split is decided by one of the strategies adopting the EMCS computation, the ICE is mainly operated in a region closer to the Optimal Operating Line (OOL), and the operating points at the lowest Brake Mean Effective Pressure (BMEP) values are avoided. It should be noted that the power split chosen by the A-V2X-ECMS strategy follows a power split logic similar to the optimal ECMS one, but without the a-priori knowledge of the entire vehicle mission profile.

6. Conclusions

In the last decade, the availability of cloud computing platforms and the introduction of look-ahead technologies, such as Vehicle-to-Everything (V2X) connectivity, have paved the way for reliable predictions of future driving conditions. In a Hybrid Electric Vehicle (HEV) framework, the exploitation of these technologies can have several benefits, ranging from enhanced safety, more efficient traffic, and better fuel economy. In this paper, information about the future vehicle driving patterns, which could be obtained from V2X connectivity, was used by a Long Short-Term Memory (LSTM) deep learning model to find the optimal equivalence factor of an innovative Adaptive Equivalent Consumption Minimization Strategy (A-ECMS) algorithm. The LSTM network was previously trained by assigning the optimal equivalence factor to a set of sequences, i.e., vehicle speed, vehicle acceleration, required power, and initial SoC, over a wide spectrum of driving conditions. The potential of the proposed algorithm was assessed over the Artemis driving cycles and in a complete real-driving scenario, following the requirements of the Real Driving Emissions (RDE) regulation. As a benchmark, the results of the proposed methodology were compared with different reference sets: a Rule-Based (RB) strategy, extracted from the experimental campaign performed on the real vehicle, an optimal ECMS, whose equivalence factor was tuned offline to ensure the charge sustainability, and a standard adaptation algorithm for the equivalence factor of the ECMS. The results demonstrate the robustness of the

proposed methodology and its versatility under several driving conditions: it guarantees charge sustainability while reaching sub-optimal results in terms of fuel consumption in all the simulated driving cycles. An additional analysis was done on the Brake Specific Fuel Consumption (BSFC) map featuring the engine working points. It was shown that the proposed strategy follows a power split logic similar to the optimal ECMS one, but without the a-priori knowledge of the entire vehicle mission profile. Finally, the strategy feasibility is proved by comparing its Real-Time (RT) factor with the ECMS one. Since this work was focused on the optimization of the energy management strategy, and not on the assessment of the V2X capabilities, a perfect knowledge of the future speed profile was assumed. Future work will investigate the impact of uncertainties related to the estimation of traffic conditions on the adaptation algorithm. Moreover, future work will be aimed at exploring the impact that V2X information can have on a charge-depleting strategy of a Plug-in Hybrid Electric Vehicle (PHEV).

CRediT authorship contribution statement

Luca Pulvirenti: Conceptualization, Methodology, Software, Writing – original draft, Visualization. **Luciano Rolando:** Conceptualization, Methodology, Supervision, Writing – review & editing. **Federico Millo:** Supervision, Writing – review & editing, Project administration.

Declaration of Competing Interest

The authors declare that they have no known competing financial interests or personal relationships that could have appeared to influence the work reported in this paper.

Acknowledgments

This research was financially supported by Regione Piemonte (Italy) under the Program L.R. 34/04–Programma d'intervento per le attivita produttive 2011/2017–Asse 3 (Internazionalizzazione), Misura 3.1 "Contratto d'insediamento". Progetto: "Sviluppo di una nuova generazione di sistemi di propulsione di veicoli ibridi ed elettrici"/"Development of a new generation of hybrid and electric propulsion systems", -Soc. FEV Italia Srl e Politecnico di Torino.

References

[1] European Commission, 'Stepping up Europe's 2030 climate ambition. Investing in a climate-neutral future for the benefit of our people," accessed October 2021, https://ec.europa.eu/commission/presscorner/detail/en/IP_21_3541https://knowledge4policy.ec.europa.eu/publication/communication-com2020562-stepping-europe%E2%80%99s-2030-climate-ambition-investing-climate_en.

[2] UNECE, "European Green Deal: commission proposes transformation of EU economy and society to meet climate ambitions," accessed October 2021, https://ec.europa.eu/commission/presscorner/detail/en/IP_21_3541.

[3] IEA, "Largest end-uses of energy by sector in selected IEA countries," 2018, Paris, accessed October 2021, https://www.iea.org/data-and-statistics/charts/largest-end-uses-of-energy-by-sector-in-selected-iea-countries-2018.

[4] ICCT, "Fit for 55: a review and evaluation of the European Commission proposal for amending the CO2 targets for new cars and vans," accessed October 2021, https://theicct.org/publications/fit-for-55-review-eu-sept21.

[5] ACEA, "Electric Vehicles: tax Benefits and Purchase Incentives," accessed October 2021, https://www.acea.auto/files/Electric_vehicles-Tax_benefits_purchase_incentives_European_Union_2020.pdf.

[6] ICCT, "Update on electric vehicle uptake in European cities," accessed October 2021, https://theicct.org/publications/ev-uptake-eu-cities-oct21.

[7] ICCT, "Europe's CO2 emission performance standards for new passenger cars: lessons from 2020 and future prospects," accessed October 2021, https://theicct.org/publications/eu-ev-pv-co2-emission-performance-sept21.

[8] ACEA, "Fuel types of new passenger cars in the EU," accessed October 2021, https://www.acea.auto/figure/fuel-types-of-new-passenger-cars-in-eu/.

[9] L. Björnsson, S. Karlsson, Electrification of the two-car household: PHEV or BEV? Transp. Res. Part C Emerg. Technol. 85 (2017) 363–376, https://doi.org/10.1016/j.trc.2017.09.021. ISSN 0968-090X.

[10] A. Sciarretta, L. Guzzella, Control of hybrid electric vehicles, IEEE Control Syst. Mag. 27 (2) (2007) 60–70, https://doi.org/10.1109/MCS.2007.338280.

[11] D. Tran, M. Vafaeipour, M. El Baghdadi, Barrero Fernandez, et al., Thorough state-of-the-art analysis of electric and hybrid vehicle powertrains: topologies and integrated energy management strategies, Renew. Sustain. Energy Rev. 119 (2020), https://doi.org/10.1016/j.rser.2019.109596.

[12] G. Paganelli, Conception Et Commande D'une Chaîne De Traction Pour Véhicule Hybride Parallèle Thermique Et électrique, Université de Valenciennes, Valenciennes, 1999. Ph.D. dissertation.

[13] L. Serrao, S. Onori, G. Rizzoni, ECMS as a realization of Pontryagin's minimum principle for HEV control, in: Proceedings of the American Control Conference, 2009, pp. 3964–3969, https://doi.org/10.1109/ACC.2009.5160628.

[14] S. Onori, L. Serrao, G. Rizzoni, Adaptive equivalent consumption minimization strategy for hybrid electric vehicles, in: Proceedings of the ASME Dynamic Systems and Control Conference, Cambridge, Massachusetts, USA 1, 2010, pp. 499–505, https://doi.org/10.1115/DSCC2010-4211.

[15] European Commission, "Cooperative, connected and automated mobility (CCAM)," accessed October 2021, https://ec.europa.eu/transport/themes/its/c-its_en.

[16] European Commission, "Commission Directive (EU) 2010/40/EU of 7 July 2010 of the European Parliament and of the Council the framework for the deployment of Intelligent Transport System in the field of road transport and for interfaces with other modes of transport," https://eur-lex.europa.eu/LexUriServ/LexUriServ.do?uri=OJ:L:2010:207:0001:0013:EN:PDF.

[17] S. Arslan, M. Saritas, The effects of OFDM design parameters on the V2X communication performance: a survey, Veh. Commun. 7 (2017) 1–6, https://doi.org/10.1016/j.vehcom.2017.01.004.

[18] G. De Nunzio, A. Sciarretta, I. Ben Gharbia, L. Ojeda, A constrained eco-routing strategy for hybrid electric vehicles based on semi-analytical energy management, in: Proceedings of the 21st International Conference on Intelligent Transportation Systems (ITSC), 2018, pp. 355–361, https://doi.org/10.1109/ITSC.2018.8569835.

[19] M. Kamal, J. Imura, T. Hayakawa, A. Ohata, et al., Traffic signal control of a road network using MILP in the MPC framework, Intell. Transp. Syst. Res. 13 (2014), https://doi.org/10.1007/s13177-014-0090-3.

[20] Gupta, S., Rajakumar Deshpande, S., Tufano, D., Canova, M. et al., "Estimation of fuel economy on real-world routes for next-generation connected and automated hybrid powertrains," SAE Technical Paper 2020-01-0593, 2020, doi:10.4271/2020-01-0593.

[21] Baker, D., Asher, Z., and Bradley, T., "V2V communication based real-world velocity predictions for improved HEV fuel economy," SAE Technical Paper 2018-01-1000, 2018, doi:10.4271/2018-01-1000.

[22] F. Zhang, J. Xi, R. Langari, Real-time energy management strategy based on velocity forecasts using V2V and V2I communications, IEEE Trans. Intell. Transp. Syst. 18 (2) (2017) 416–430, https://doi.org/10.1109/TITS.2016.2580318.

[23] Hou, S.,Yin, H., Ma, Y., and Gao, J., "Energy management strategy of hybrid electric vehicle based on ecms in intelligent transportation environment", Volume 54, Issue 10, Pages 157–162, 2021, 10.1016/j.ifacol.2021.10.157.

[24] P. Wang, J. Li, Y. Yu, X. Xiong, et al., Energy management of plug-in hybrid electric vehicle based on trip characteristic prediction, Proc. Inst. Mech. Eng. Part D J. Autom. Eng. 234 (2020), https://doi.org/10.1177/0954407020904464, 095440702090446.

[25] A. Shrestha, A. Mahmood, Review of deep learning algorithms and architectures, IEEE Access (2019), https://doi.org/10.1109/ACCESS.2019.2912200, 1-1.

[26] Z. Chen, Y. Liu, Y. Zhang, Z. Lei, et al., A neural network-based ECMS for optimized energy management of plug-in hybrid electric vehicles, Energy (2021), 122727, https://doi.org/10.1016/j.energy.2021.122727.

[27] Z. Wei, Y. Zhang, A real-time energy management strategy of hevs based on velocity prediction, in: Proceedings of the 60th Annual Conference of the Society of Instrument and Control Engineers of Japan (SICE), 2021, pp. 490–494.

[28] M. Haußmann, D. Barroso, C. Vidal, L. Bruck, A. Emadi, A novel multi-mode adaptive energy consumption minimization strategy for P1-P2 hybrid electric vehicle architectures, in: Proceedings of the IEEE Transportation Electrification Conference and Expo (ITEC), 2019, pp. 1–6, https://doi.org/10.1109/ITEC.2019.8790525.

[29] Y. Yong, S. Xiaosheng, H. Changhua, Z. Jianxun, A review of recurrent neural networks: LSTM cells and network architectures, Neural Comput. 31 (2019) 1235–1270, https://doi.org/10.1162/neco_a_01199. Massachusetts Institute of Technology.

[30] S. Hochreiter, J. Schmidhuber, Long short-term memory, Neural Comput. 9 (8) (1997) 1735–1780, https://doi.org/10.1162/neco.1997.9.8.1735.

[31] J. Pérez-Ortiz, F.A. Gers, D. Eck, J. Schmidhuber, Kalman filters improve LSTM network performance in problems unsolvable by traditional recurrent nets, Neural Netw. 16 (2) (2003) 241–250, https://doi.org/10.1016/S0893-6080(02)00219-8.

[32] Y. Chen, Y. Wang, Z. Dong, J. Su, et al., 2-D regional short-term wind speed forecast based on CNN-LSTM deep learning model, Energy Convers. Manag. 244 (2021), 114451, https://doi.org/10.1016/j.enconman.2021.114451.

[33] F. Millo, L. Rolando, L. Tresca, L. Pulvirenti, Development of a neural network-based energy management system for a plug-in hybrid electric vehicle, Transp. Eng. 11 (2023), 100156, https://doi.org/10.1016/j.treng.2022.100156. ISSN 2666-691X.

[34] F.A. Gers, J. Schmidhuber, F. Cummins, Learning to forget: continual prediction with LSTM, Neural Comput. 12 (10) (2000) 2451–2471, https://doi.org/10.1162/089976600300015015.

[35] F. Millo, L. Rolando, L. Pulvirenti, G. DiPierro, A methodology for the reverse engineering of the energy management strategy of a plug-in hybrid electric vehicle for virtual test rig development, SAE Int. J. Electrified Veh. (2021), https://doi.org/10.4271/14-11-01-0009.

[36] DiPierro, G., Galvagno, E., Mari, G., Millo, F. et al., "A reverse-engineering method for powertrain parameters characterization applied to a P2 plug-in hybrid electric

vehicle with automatic transmission," SAE Technical Paper, 2020-37-0021, 2020, doi:10.4271/2020-37-0021.
[37] UNECE, "UNECE Regulation N°83 - Revision 5. Uniform provisions concerning the approval of vehicles with regard to the emissions of pollutants according to the engine fuel requirements," Geneva, 2015, https://tinyurl.com/cxmdcdzy.
[38] UNECE, "UNECE Global technical regulation No. 15 Worldwide Harmonized Light Vehicles Test Procedure," Geneva, 2015, https://tinyurl.com/859eyr6c.
[39] European Commission, "Commission Regulation (EU) 2017/1151 of 1 June 2017 of the European Parliament and of the Council on type-approval of motor vehicles with respect to emissions from light passenger and commercial vehicles (Euro 5 and Euro 6) ...", 2017, https://tinyurl.com/53ecjp7s.
[40] GT-SUITE, "Vehicle Driveline and HEV Application Manual," v 2021, Gamma Technologies LLC.
[41] F. Millo, L. Rolando, M. Andreata, Numerical simulation for vehicle powertrain development, Awrejcewicz, J.. Numerical Analysis—Theory and Application, InTech, 2011, https://doi.org/10.5772/24111.
[42] EPA, "Dynamometer drive schedules," accessed October 2021, https://www.epa.gov/vehicle-and-fuel-emissions-testing/dynamometer-drive-schedules.
[43] NRETS - Institut National de Recherche sur les Transports et leur Securite, "Real-World Driving Cycles for Measuring Cars Pollutant Missions - Part A: the ARTEMIS European Driving Cycles," Report INRETS-LTE 0411, June 2004.
[44] DieselNet, "RTS 95 Cycle," accessed October 2021, https://dieselnet.com/standards/cycles/rts95.php.
[45] S. Onori, L. Serrao, G. Rizzoni, Hybrid Electric Vehicles: Energy Management Strategies, Springer, 2016. ISBN:978-1-4471-6781-5.
[46] MATLAB, Statistics and Machine Learning Toolbox User's Guide, The MathWorks Inc, Natick, Massachusetts, 2021 version 9.9 (R2021a).
[47] A. David, S. Vassilvitskii, K-means++: the advantages of careful seeding, in: Proceedings of the 18th Annual ACM-SIAM Symposium on Discrete Algorithms SODA '07:, 2007, pp. 1027–1035, https://doi.org/10.1145/1283383.1283494.
[48] H. Abdi, L. Williams, Principal component analysis, Wiley Interdiscip. Rev. Comput. Stat. 2 (2010) 433–459, https://doi.org/10.1002/wics.101, doi:10.1002/wics.101.
[49] MATLAB, "Experiment manager," 2021, online documentation, https://it.mathworks.com/help/deeplearning/ref/experimentmanager-app.html.